Bulletin of the Seismological Society of America, Vol. 102, No. 6, pp. 2727–2740, December 2012, doi: 10.1785/0120120018

Validation of Ground-Motion Simulations for Historical Events Using SDoF Systems

by C. Galasso, F. Zareian, I. Iervolino, and R. W. Graves

Abstract The study presented in this paper is among the first in a series of studies toward the engineering validation of the hybrid broadband ground-motion simulation methodology by Graves and Pitarka (2010). This paper provides a statistical comparison between seismic demands of single degree of freedom (SDoF) systems subjected to past events using simulations and actual recordings. A number of SDoF systems are selected considering the following: (1) 16 oscillation periods between 0.1 and 6 s; (2) elastic case and four nonlinearity levels, from mildly inelastic to severely inelastic systems; and (3) two hysteretic behaviors, in particular, nondegrading–nonevolutionary and degrading–evolutionary. Demand spectra are derived in terms of peak and cyclic response, as well as their statistics for four historical earthquakes: 1979 M_w 6.5 Imperial Valley, 1989 M_w 6.8 Loma Prieta, 1992 M_w 7.2 Landers, and 1994 M_w 6.7 Northridge.

The results of this study show that both elastic and inelastic demands from simulated and recorded motions are generally similar. However, for some structural systems, the inelastic response to simulated accelerograms may produce median demands that appear different from those obtained using corresponding recorded motions. The magnitude of such differences depends on the SDoF period, the nonlinearity level, and, to a lesser extent, the hysteretic model used. In the case of peak response, these discrepancies are likely due to differences in the spectral shape, while the differences in terms of cyclic response can be explained by some integral parameters of ground motion (i.e., duration-related). Moreover, the intraevent standard deviation values of structural demands calculated from the simulations are generally lower than those given by recorded ground motions, especially at short periods. The assessment of the results using formal statistical hypothesis tests indicates that, in most cases, the differences found are not significant, increasing the trust in the use of simulated motions for engineering applications.

Introduction and Motivation

The use of nonlinear dynamic analysis (NLDA) for assessing existing structures and designing new ones requires the availability of reliable ground-motion signals (hereinafter called ground motions or GMs). Usually, GMs are selected and scaled from a database of existing records to represent target seismic characteristics (e.g., hazard level, magnitude, source-to-site distance, and local soil conditions). Numerous methods for such selection and scaling have been proposed. A summary of the available selection and scaling methods for GMs can be found in Haselton (2009). Moreover, some advanced tools are making possible the use of recorded GMs in both research and practice (e.g., Iervolino, Galasso, and Cosenza, 2010; Iervolino *et al.*, 2011).

The inherent scarcity or total absence of suitable real GMs (e.g., recorded during past earthquakes) for some specific scenarios (e.g., large-magnitude strike-slip events recorded at close source-to-site distances) makes the use of alternative options unavoidable. This is the case, for example, for seismically active regions (e.g., California), where the spectral accelerations of interest are often relatively large and the hazard-controlling earthquake scenarios are typically large-magnitude events on nearby faults. More generally, the recently released American Society of Civil Engineering (ASCE) Standard ASCE/SEI 7-10 (ASCE, 2010) explicitly states that, in performing NLDA, "where the required number of appropriate recorded ground motion records are not available, appropriate simulated ground motions shall be used to make up the total number required."

Physics-based simulated (or synthetic) GMs capturing complex source features (such as spatially variable slip

distributions, rise time, and rupture velocities), path effects (geometric spreading and crustal damping), and site effects (wave propagation through basins and shallow site response) provide a valuable supplement to recorded GMs, fulfilling a variety of engineering needs (Somerville, 1993). Other alternatives include stochastic-based artificial accelerograms (e.g., Vanmarcke *et al.*, 1997; Rezaeian and Der Kiureghian, 2011) and modified real records matching a given elastic target spectrum (Atkinson and Goda, 2010; Iervolino, De Luca, and Cosenza, 2010).[1] Among engineers, the general concern is that simulated records may not be equivalent to real records in estimating seismic demand and, hence, in estimating the induced damages to structures (Naeim and Graves, 2006). Moreover, synthetic GMs are not yet widely available in engineering practice, especially in regions where seismogenic fault locations and characteristics and the regional velocity structure are not established. In California, the recently released Southern California Earthquake Center (SCEC) Broadband Platform (see Data and Resources) provides scientists and engineers with a suite of tools to compute broadband synthetic ground motions, including the effects of heterogeneous rupture propagation and nonlinear site effects. These capabilities continue to be refined as additional studies, such as the present one, provide improved methodologies.

To validate synthetic GMs, some previous and concurrent studies have employed a direct (i.e., by visual inspection) comparison between observed and simulated waveforms (especially in the case of low-frequency waveforms) or a comparison between median levels of observed and simulated intensity measures (including elastic spectral ordinates) for hybrid broadband simulation procedures (Olsen *et al.*, 2003; Graves and Pitarka, 2010). Baker and Jayaram (2008) compared the statistical properties of simulated and recorded GMs, with a focus on the correlation of elastic spectral values at multiple periods and on the spatial correlation of GM intensity measures, showing that the simulations agree with the observations, especially when soft-soil sites are excluded. Olsen and Mayhew (2010) have recently proposed a goodness-of-fit criterion for broadband synthetic seismograms using several intensity measures (including duration) and the ratio between the inelastic and elastic response spectra. They present an application to the very well recorded 2008 M_w 5.4 Chino Hills, California, earthquake, suggesting that simulated GMs can be used effectively for moderate and long-period structures. Recently, Star *et al.* (2011) compared elastic acceleration spectral ordinates (at several periods) from simulated motions for an M_w 7.8 rupture scenario on the San Andreas fault (two permutations with different hypocenter locations) and an M_w 7.15 Puente Hills blind thrust scenario, to median and dispersion predictions from empirical Next Generation Attenuation (NGA) ground-motion prediction equations (GMPEs). However, the identified discrepancies between the results can indicate problems with the simulations, the GMPEs, or perhaps both.

In this study, we take a step forward and try to understand whether simulated GMs are comparable to real records in terms of their nonlinear response in the domain of SDoF systems. Such an investigation is a proxy to compare the damage potential between simulated and recorded motions for many real structural types. Similarly, Bazzurro, Sjoberg, and Luco (2004) have examined engineering validation in terms of elastic and inelastic SDoF structural response to seven suites of synthetic records that emulate the real GMs recorded at 20 stations located within 20 km from the Northridge fault rupture. The results show that six out of seven simulation methods appear to be biased, especially in the short-period range, both in the linear elastic and in the nonlinear postelastic regimes.

As the postelastic dynamic response of a structure is fundamentally important in performance-based earthquake engineering, the study presented in this paper focuses on the engineering validation of GM simulation in terms of peak and cyclic demands of inelastic SDoF systems with different elastic and hysteretic characteristics. More specifically, the study considers two kinds of SDoF systems by comparing their nonlinear response to simulated and recorded motions: (1) nondegrading–nonevolutionary and (2) degrading–evolutionary. Demand spectra, in terms of inelastic displacement and equivalent number of cycles, are derived for different elastic periods and strength factors, considering the hybrid broadband simulation methodology by Graves and Pitarka (2010) for four historical Californian earthquakes (see Description of Synthetic and Real Ground-Motion Datasets). In fact, past events provide an important opportunity to test the ability to use the hybrid broadband GM simulation to generate synthetic GMs consistent with those observed. On a broader perspective, the hybrid broadband simulation provides a complete prescription for simulating motions for future earthquakes, including extrapolation to those beyond the magnitude range considered in the current set of validation events (Graves and Aagaard, 2011).

The aim here is to address, on a statistical basis, whether simulated GMs are systematically biased in terms of their median nonlinear response characteristics in comparison with real records. We also look at the dispersion (i.e., intra-event variability) of response to recorded and simulated GMs. Hypothesis tests on selected samples are carried out to quantitatively assess the statistical significance of the results in terms of both peak and cyclic response. Finally, the sensitivity of the results to source-to-site distances, soil conditions, and GM durations is investigated.

The results from this study highlight the similarities and differences between synthetic and real records. These similarities should provide trust in using the simulation

[1]Modified recorded motions may distort the source and path effect on the waveform from reality, which can result in records that are less realistic than the motions from physics-based simulations. However, some studies have shown that modified accelerograms may be acceptable with respect to bias in structural nonlinear response with respect to recorded GMs (e.g., Iervolino, De Luca, and Cosenza, 2010).

methodology for engineering applications, while the discrepancies, if statistically significant, should help in improving the generation of synthetic records.

Description of Synthetic and Real Ground-Motion Datasets

Graves and Pitarka (2010) developed a hybrid broadband (0–10 Hz) GM simulation methodology that combines a physics-based deterministic approach at low frequency ($f \leq 1$ Hz; i.e., $T \geq 1$ s) with a semistochastic approach at high frequency ($f > 1$ Hz; i.e., $T < 1$ s). The low- and high-frequency waveforms are computed separately and then combined to produce a single time history through a matching filter. At frequencies below 1 Hz, the methodology contains a theoretically rigorous representation of fault rupture and wave propagation effects and attempts to reproduce recorded GM waveforms and amplitudes. At frequencies above 1 Hz, waveforms are simulated using a stochastic representation of source radiation combined with a simplified theoretical representation of wave propagation and scattering effects. The reason for using different simulation approaches for the different frequency bands is because of the seismological observation that source radiation and wave propagation effects tend to become stochastic at frequencies of about 1 Hz and higher, primarily reflecting the relative lack of knowledge about the details of these phenomena at higher frequencies. For both short and long periods, the effect of relatively shallow site conditions, as represented by shear-wave velocity in the upper 30 m, V_{S30}, is accounted for using the empirical site amplification model by Campbell and Bozorgnia (2008).

The present study uses four historical earthquakes modeled by Graves and Pitarka (2010): 1979 M_w 6.5 Imperial Valley, 1989 M_w 6.8 Loma Prieta, 1992 M_w 7.2 Landers, and 1994 M_w 6.7 Northridge. The only earthquake-specific input parameters used in the simulation process are the seismic moment, the overall fault dimensions and geometry, the hypocenter location, and a smoothed representation of the final slip distribution. All other required source parameters (e.g., rupture propagation time, rise time, slip function, and fine-scale slip heterogeneity) are developed using the scaling relations presented by Graves and Pitarka (2010). The methodology provides a reliable framework for generating rupture descriptions for future earthquakes, as demonstrated by Graves and Aagaard (2011).[2] Complete details of the rupture generation procedure are given in Graves and Pitarka (2010). For each simulated event, the model region covers a wide area surrounding the fault, including many strong-motion recording sites available in the NGA database: 33 for Imperial Valley, 71 for Loma Prieta, 23 for Landers, and 133 for Northridge. These sites are shown with triangles in Figure 1.

This study uses a limited number of sites mentioned in the previous paragraph, considering only those that have real recordings with a usable bandwidth larger than 0.1–8 s. This limitation yields a total of 126 sites for the entire study. These sites are marked with filled triangles in Figure 1. Such a large bandwidth for recorded motions provides a justifiable means of covering a good range of nonlinear SDoF systems where nonlinear response is sensitive to spectral ordinates beyond the fundamental period. In some cases, especially for degrading–evolutionary SDoF systems, the usable lower frequency will tend to be somewhat higher (more restrictive); see Bazzurro, Sjoberg, Luco, *et al.* (2004) for a discussion of this topic. Therefore, the analysis and results presented in this paper refer to structures with fundamental periods less than 6 s. The fact that recorded data are often unusable at high periods provides another justification for using synthetic motions.

Description of the SDoF Systems and Demand Measures

The pool of GMs described in the Description of Synthetic and Real Ground-Motion Datasets section, recorded and simulated, is used to perform NLDAs on a total of 272 SDoF systems, representing combinations of variations in three parameters:

- SDoF fundamental period, T: this study considers periods between 0.1 and 6 s. The period range is sampled with a step of 0.1 s between 0.1 and 0.5 s, a step of 0.25 s between 0.5 and 1 s, a step of 0.5 s between 1 and 5 s, and a step of 1 s between 5 and 6 s.
- Strength reduction factors, R: this parameter is the ratio of the GM elastic force to the yield strength of the SDoF system, F_y. R is varied in order to describe elastic–inelastic structural behavior from elastic ($R = 1$), for completeness and checking purposes, to mildly inelastic ($R = 2$) and severely inelastic structures ($R = 8$).
- Hysteretic behavior: this study considers four hysteretic behaviors, that is, two variations of two basic models, nondegrading–nonevolutionary and degrading–evolutionary. A nondegrading elastic–plastic with positive strain-hardening, α, model (EPH) represents the nondegrading–nonevolutionary SDoF system (Fig. 2a); two values of α, that is, 3% and 5%, are considered. The degrading–evolutionary SDoF system (ESD) comprises a negative strain hardening (i.e., a softening branch), $-\alpha$, and a residual strength of $\alpha \cdot F_y$; also, in this case, two α values, 5% and 10%, are considered. The simple peak-oriented model is considered in order to account for the cyclic stiffness degradation, while cyclic deterioration of strength is not considered (Ibarra *et al.*, 2005); see Figure 2b. All ESD systems have ductility before reaching the residual

[2]In particular, in the case of a future event, the input parameters for the simulation can either be reliably estimated (e.g., seismic moment and fault dimensions) or parametrically assessed using multiple realizations (e.g., hypocenter location and slip distribution). All other source parameters can be determined using the scaling relations described in Graves and Pitarka (2010).

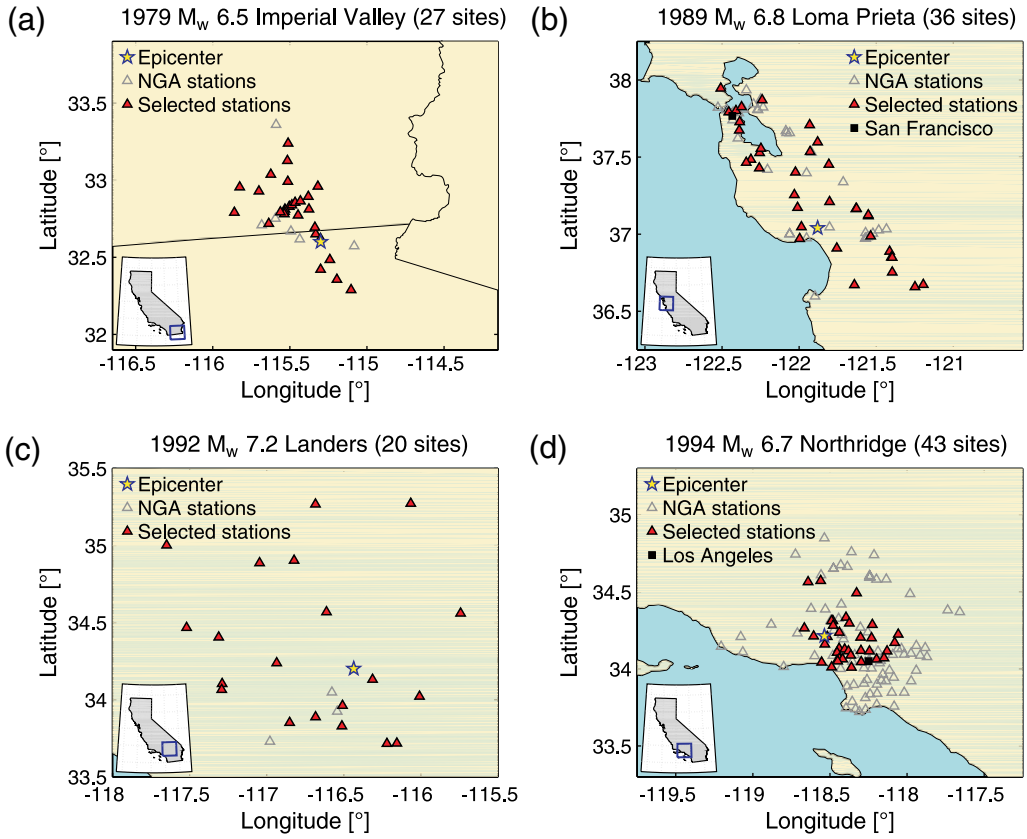

Figure 1. Maps of the earthquakes considered. The star is the epicenter, and the triangles are the recording stations in the NGA database for which the simulations are available. The filled triangles are the recording stations considered in this study. (b) San Francisco and (d) Los Angeles are also indicated on the map (squares). The color version of this figure is available only in the electronic edition.

strength, evaluated as the ratio between ultimate displacement, Δ_u, and yielding displacement, Δ_y, in the backbone curve (i.e., a ductility limit), equal to 5 and 10 (for α equal to 5% and 10%, respectively). A mass-proportional viscous damping coefficient corresponding to a 5% critical damping ratio is used and kept constant throughout the time history analyses.

It is worth noting that the peak value of the elastic base shear, or equivalently the peak elastic deformation, experienced by an elastic structure is a GM-specific quantity. Therefore, one can achieve the same value of R either (a) for each record in a dataset or (b) in an average sense for all of the records in the same dataset. We will call case (a) the constant-R approach. In this case, the same target R value can be achieved by varying the yield strength of the structure, F_y, from record to record. More precisely, for each record, F_y is proportional to the elastic spectral acceleration for that record (at the fundamental period for the system) divided by the desired value of R. This set of analyses effectively applies each record to SDoF systems with slightly different strength characteristics. We will call case (b) the constant-strength approach. In this case, the same R value can be obtained by keeping F_y constant. In this way, the same structure, with an average strength (for example,

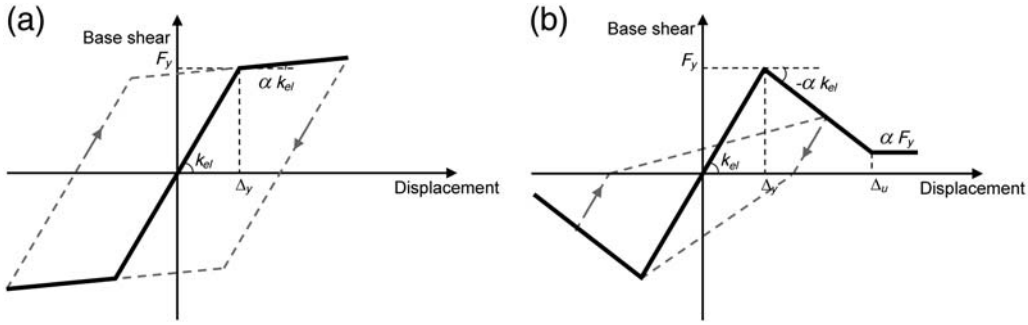

Figure 2. (a) EPH backbone curve and (b) ESD backbone curve.

based on a given matched target spectrum) that varies with any given period and R value, is used to evaluate the nonlinear response to all of the records. In this study, we considered the constant-R approach to account for the large variability of the GM features (e.g., in terms of spectral ordinates) and to guarantee the expected levels of nonlinearity. Obviously, the results obtained from the constant-R approach may differ from those obtained using a constant-strength approach. However, a similar study by Bazzurro, Sjoberg, and Luco (2004) showed that the results of the comparison between recorded and simulated GMs using the constant-strength and the constant-R approaches for several SDoF systems do not differ significantly.

This investigation considers two representations of SDoF response, that is, two engineering demand parameters (EDPs): inelastic displacement, $\Delta_{\text{inelastic}}$, and equivalent number of cycles, N_e. These two parameters are considered in order to investigate both the peak displacement demand and the cyclic seismic response; in particular, the N_e parameter well captures GM potential effects on structural response in terms of dissipated hysteretic energy.

Using the adopted constant-R approach, $\Delta_{\text{inelastic}}$ for each GM is computed from the dynamic response of the SDoF systems considered (characterized by given values of T and R), using specific levels of yielding strength relative to the strength required to keep the system elastic (peak elastic base shear) as shown in equation (1), where m is the mass of the system and SA is the spectral acceleration corresponding to the GM considered at the same period (i.e., considering a system with the same mass and initial stiffness).

$$F_y = \frac{m \cdot \text{SA}(T)}{R}. \tag{1}$$

N_e is given by the cumulative hysteretic energy, E_H, evaluated as the sum of the areas of the hysteretic cycles (not considering the contribution of viscous damping) normalized with respect to the largest cycle, and evaluated as the area underneath the monotonic backbone curve from the yielding displacement to the peak inelastic displacement A_{plastic} (see equation 2).

$$N_e = \frac{E_H}{A_{\text{plastic}}}. \tag{2}$$

Values of N_e close to 1 indicate the presence of a large plastic cycle in the nonlinear response, while high values of N_e indicate the presence of many plastic cycles; N_e generally decreases with period in the short-period range and increases with R (Manfredi, 2001). In addition, N_e varies largely depending on the GM features, from values close to 1 for impulsive earthquakes to a value of about 40 for long-duration earthquakes.

Other parameters widely used in similar studies are the inelastic displacement ratio, C_R (i.e., $\Delta_{\text{inelastic}}$ at a given period and for a given value of R, normalized with respect to peak elastic displacement, S_d, at the same period), and the displacement ductility, D_{kin} (i.e., the ratio between $\Delta_{\text{inelastic}}$ and Δ_y, the yielding displacement). However, the constant-R approach used in this study, and the absence of a given matched target spectrum by simulated and recorded GMs, can lead to large differences between C_R and D_{kin} for the two datasets for each earthquake. These differences are mostly due to the assumptions of the analytic approach (e.g., the constant-R approach) and not to shortcomings of the simulation procedure.

Results and Discussion

All GMs (recorded and simulated) selected for each earthquake event are used as input for NLDA applied to all of the SDoF systems considered, yielding a total of 64,000 NLDAs performed. Only the horizontal components of GMs (i.e., north–south [NS] and east–west [EW]) are used, while the vertical component is neglected. The spectral responses for the two horizontal components at each station are computed and then combined into an average spectral response using the geometric mean. For each earthquake and each EDP ($\Delta_{\text{inelastic}}$ and N_e), the median value (i.e., the exponential of the mean of the natural log of the EDP across all of the available stations) for the synthetic records divided by the median value for the real dataset is computed and plotted across the period range being considered (for different R values). A ratio above unity, if statistically significant, means that the simulations overestimated the response, and the opposite is true if the ratio is smaller than 1.

For instance, a ratio of the medians of $\Delta_{\text{inelastic}}$ obtained using synthetics and recorded motions that is larger than one indicates that the synthetic records tend to produce, on average, systematically more damaging nonlinear spectral displacements than real records. Conversely, deviations below unity indicate that the simulated records tend to be, on average, more benign in producing nonlinear responses than those in nature.

In order to provide a measure of inherent intraevent variability in the simulations compared with that of real GMs, the ratio of the standard deviation of the natural log of the data (simply log-standard deviation hereinafter)[3] for simulated and recorded GMs (for all sites and distances of a given earthquake) is plotted as a function of the period and R. A line above unity means that the simulated GMs produced more record-to-record variability, whereas the opposite is true for a line below one.

A direct comparison of response statistics is acceptable, as the simulated datasets are developed to match exactly the same earthquakes and site conditions (i.e., at the same stations) of the real recordings.

[3]This choice is useful for performing parametric hypothesis tests (discussed subsequently in this paper). It is worth reminding that the log-standard deviation of the EDPs data is approximately equal to the coefficient of variation (CoV) of the EDPs data. Only if the synthetic and recorded GMs generate seismic demands characterized by the same mean values, the results for the comparison in terms of log-standard deviations can be extended to the comparison in terms of standard deviations (in the original scale).

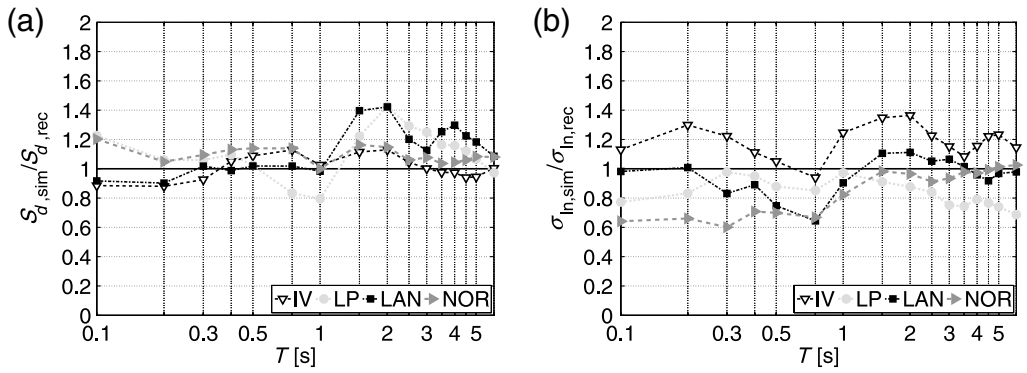

Figure 3. Ratios of the (a) medians and (b) log-standard deviations of the elastic displacement spectra for simulated GMs to the corresponding quantities computed for the recorded GMs. In this figure, IV represents the Imperial Valley event, LP represents the Loma Prieta event, LAN represents the Landers event, and NOR represents the Northridge event.

Comparison between Statistical Measures of Elastic Response Spectra

Elastic response spectra provide succinct features of the peak response for the linear elastic SDoF systems to strong GMs and often are used as a seismic intensity measure for a broad range of purposes. For each of the four events considered in this study, the median value of the elastic displacement spectral ordinates for the simulated records divided by the median value for the recorded dataset is computed and plotted across the period range considered (see Fig. 3a). In general, the elastic spectra of the simulated waveforms agree reasonably well with the observations.

In particular, in the case of the Imperial Valley and the Northridge earthquakes, the model bias (i.e., the considered ratios' departure from unity) is near zero ($< \pm 20\%$) across the entire bandwidth, indicating that the simulations are accurately reproducing the main characteristics of the observed GMs, with a slight overestimation. For the Landers event, the model bias is larger (about 40%) across the frequency range (1.5–5 s). Hypothesis tests (discussed subsequently in this paper) do not confirm these differences to be statistically significant. For the Loma Prieta event, some differences are evident around a period of 2 s (with a bias of about 40%); nevertheless, again, hypothesis tests confirm that these differences are not statistically significant.

The curves in Figure 3a make it clear that not only the median spectral amplitudes but also the spectral shapes for simulated GMs can be different than the median response spectrum from the real recordings. In fact, in the median ratios shown in Figure 3a, any trend across the periods that departs from a horizontal line suggests that the elastic spectra generated by the synthetic model have, on average, a different shape than those produced by nature. The difference in spectral shape is large, especially for the Loma Prieta and Landers events, for a wide range of periods. These differences in spectral shape may influence the nonlinear response statistics at all strength levels (e.g., Luco and Bazzurro, 2007).

Except for the Imperial Valley event, the real record log-standard deviations of the spectra are generally larger than those of the simulated GMs, particularly at the shorter periods (Fig. 3b). This trend of relatively low intraevent variability in the simulations, especially at short periods, has been noted previously by Star *et al.* (2011).

To address this issue, Stewart *et al.* (2011) recently proposed a revision to the simulation approach that incorporates greater stochastic variability in the high-frequency portion, although this revision has not yet been applied to the simulations considered in the current analysis. For the Imperial Valley event, the log-standard deviation of the response to simulated records is larger than that of recorded GMs across the entire period range; the considered ratio is almost constant and above unity. At long periods, this likely can be attributed to the presence in the simulated dataset of GMs featuring strong coherent velocity pulses and then large elastic response, as discussed later. Moreover, at short periods, these differences reflect the relative complexity of the regional velocity structures where the event occurred and probably some inadequacies in the velocity model used in the simulation (and the assumed anelastic attenuation function; Graves and Pitarka, 2010).

Comparison between Statistical Measures of Inelastic Response Spectra

Figure 4a shows the ratio of the median spectrum in terms of $\Delta_{\text{inelastic}}$ from the simulated GMs to the median spectrum (again in terms of $\Delta_{\text{inelastic}}$) from the recorded GMs for Imperial Valley (for the considered periods and nonlinearity levels); Figure 4b shows the same ratio in terms of N_e (same event). Figure 4c shows the ratio of the log-standard deviation of the data from the simulated GMs in terms of $\Delta_{\text{inelastic}}$ to the log-standard deviation of the data from the recorded GMs (again in terms of $\Delta_{\text{inelastic}}$); and Figure 4d shows the same ratio in terms of N_e. Figure 4 refers to the EPH (nondegrading, nonevolutionary) systems with $\alpha = 3\%$. Figures 5–7 are developed in the same fashion as Figure 4 but for Loma Prieta, Landers, and Northridge, respectively. To save space, results for the EPH systems with

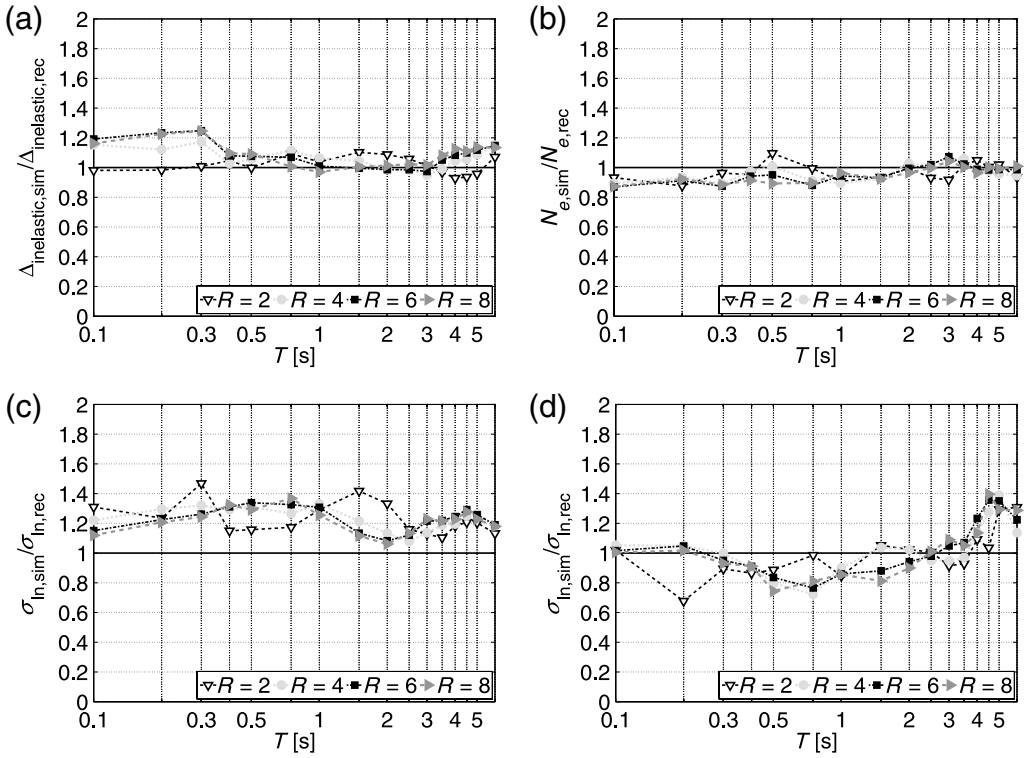

Figure 4. Ratios of the (a, b) medians and (c, d) log-standard deviations of the inelastic spectra (in terms of $\Delta_{\text{inelastic}}$ and N_e) for simulated GMs to the corresponding quantities computed for the recorded GMs for the Imperial Valley earthquake (EPH model, $\alpha = 3\%$).

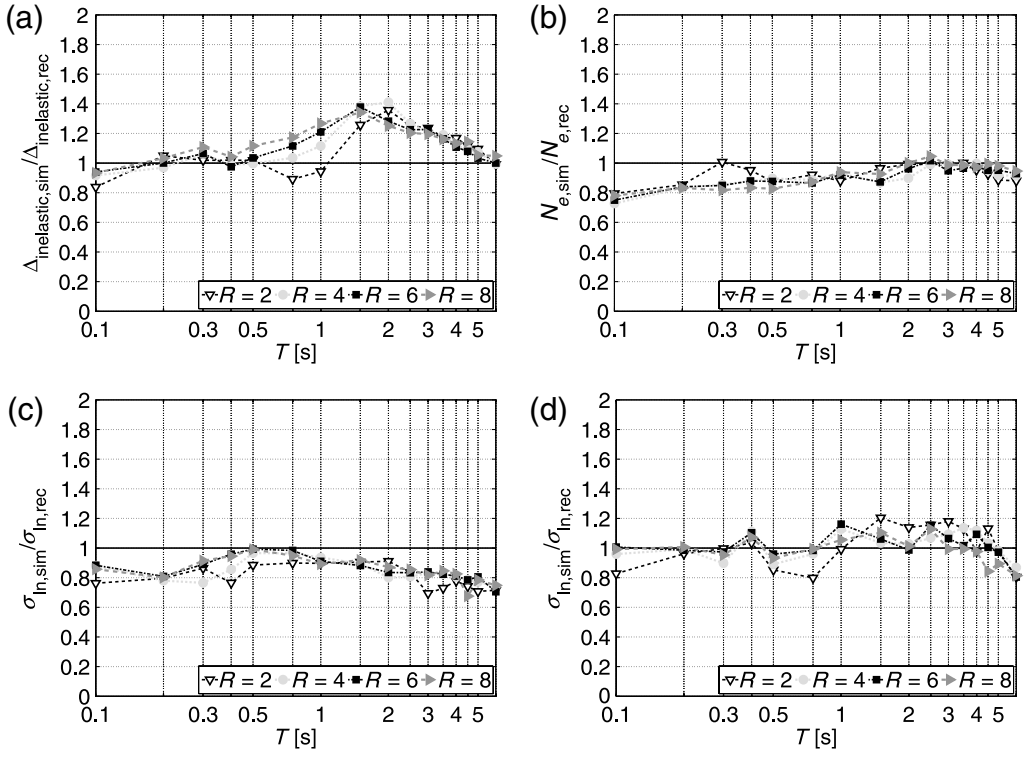

Figure 5. Ratios of the (a, b) medians and (c, d) log-standard deviations of the inelastic spectra (in terms of $\Delta_{\text{inelastic}}$ and N_e) for simulated GMs to the corresponding quantities computed for the recorded GMs for the Loma Prieta earthquake (EPH model, $\alpha = 3\%$).

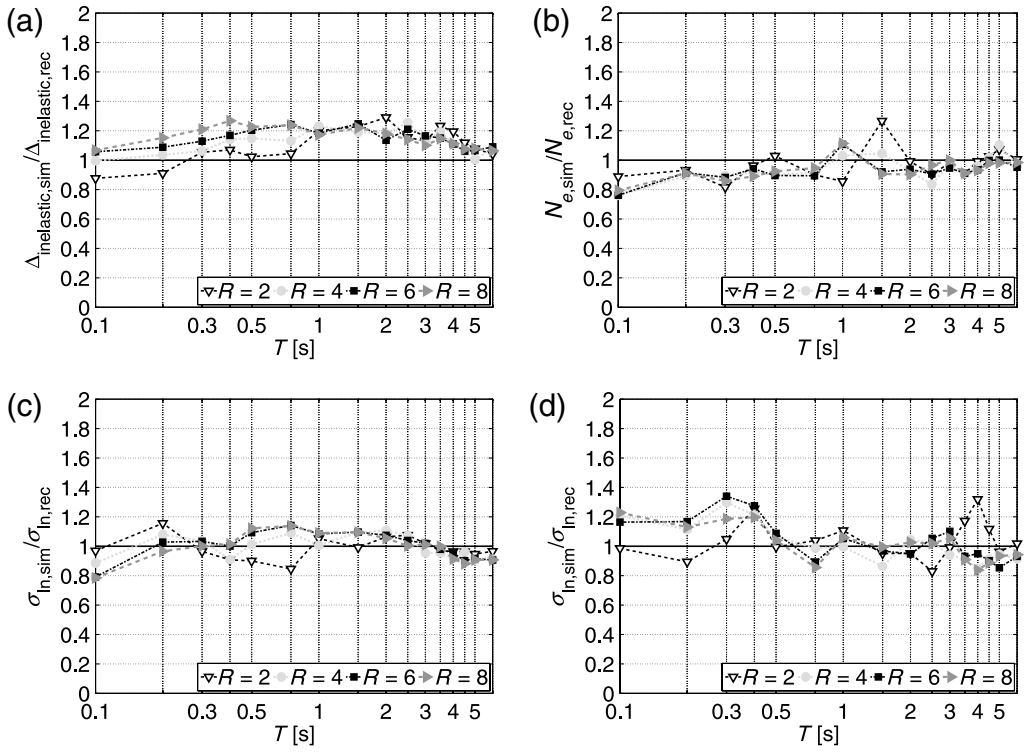

Figure 6. Ratios of the (a, b) medians and (c, d) log-standard deviations of the inelastic spectra (in terms of $\Delta_{\text{inelastic}}$ and N_e) for simulated GMs to the corresponding quantities computed for the recorded GMs for the Landers earthquake (EPH model, $\alpha = 3\%$).

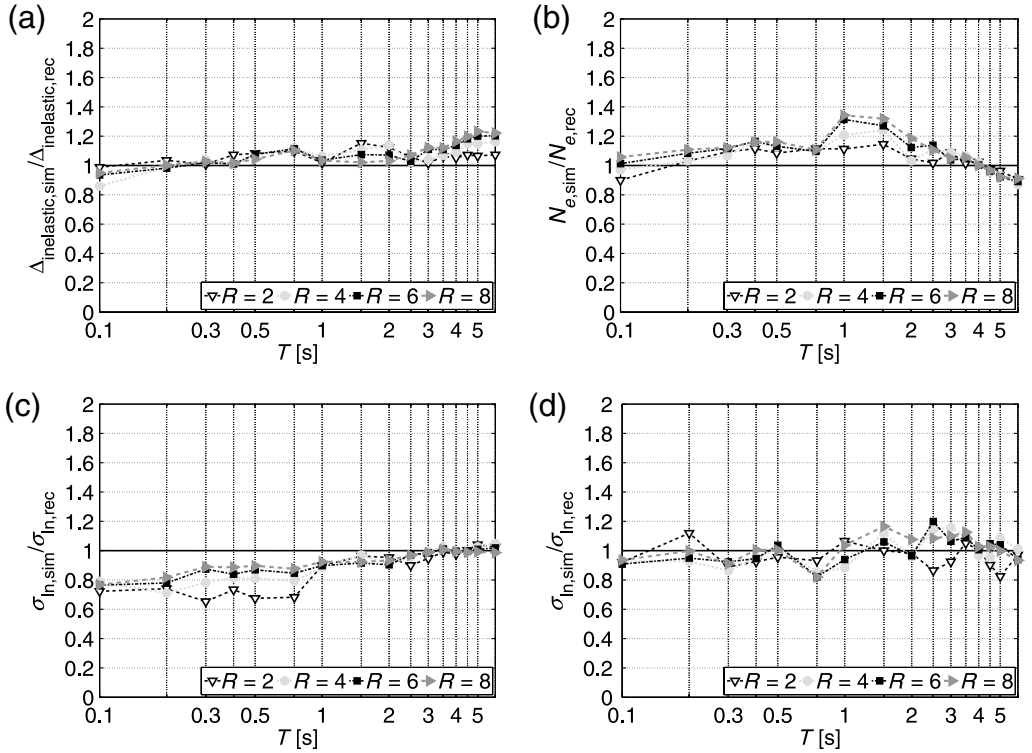

Figure 7. Ratios of the (a, b) medians and (c, d) log-standard deviations of the inelastic spectra (in terms of $\Delta_{\text{inelastic}}$ and N_e) for simulated GMs to the corresponding quantities computed for the recorded GMs for the Northridge earthquake (EPH model, $\alpha = 3\%$).

$\alpha = 5\%$ and ESD systems are not shown; similar observations can be drawn for these cases.

Looking at the postelastic response in terms of $\Delta_{\text{inelastic}}$, the bias in the estimation of the seismic demands of the SDoF system depends on the considered event, period, and strength level. Results are very similar for both the EPH and ESD systems, although for the ESD systems, the differences are slightly larger and more R-dependent. Deviations seem to be concentrated in the zone of semistochastic simulation (at very short periods), around 1 s for some cases, and at very long periods (especially at high nonlinearity levels). The fact that the bias in peak response is close to zero in the moderate-long periods of the inelastic spectra is essentially due to the equal displacement rule (Veletsos and Newmark, 1960) and is quite well observed for both recorded and simulated GMs. The observed differences at given periods are likely due to systematic differences in the average shape around those periods of the linear response spectra generated by synthetic and real GMs (Fig. 3). In fact, when the response of the SDoF system becomes severely nonlinear, its effective vibration period lengthens significantly, especially at short periods, and therefore it becomes dependent on the frequency content of the record in a fairly large bandwidth and not only in the neighborhood of the initial elastic period of vibration. For example, this is true in the case of Loma Prieta (Fig. 5), where the signature of the elastic results is evident (Fig. 3).

The results in terms of N_e show that the bias is near zero across the entire bandwidth, indicating that the simulations accurately reproduce the energy demands of the observed GMs. A certain systematic underestimation for simulated GMs is evident at short periods for Imperial Valley, Loma Prieta, and Landers, while simulated GMs tend to overestimate the cyclic response in the case of Northridge, especially around 1 s.

As in the elastic case, simulated records tend to produce nonlinear demands that are generally less variable (i.e., a lower intraevent variability is observed) compared with those produced by real records, especially at short periods, although some exceptions exist, especially in terms of N_e. From a practical standpoint, if an engineer seeks to design a new structure or assess an existing one's safety against collapse using simulated records, which tend to generate less variable response, he or she would underestimate the likelihood of extreme response values and, therefore, the probability of collapse. As in the case of elastic displacement spectra, simulated and recorded GM variability in nonlinear demands varies with the structural period, the level of nonlinearity, and the particular earthquake event.

Statistical Significance of the Differences between SDoF Demands for Simulated and Recorded Historical Motions

Parametric hypothesis tests are performed to quantitatively assess the statistical significance of the results found in median response (for each oscillation period in the considered range, each R value, and each nonlinear model) to recorded and simulated GMs, that is, to assess whether the analyzed ratios differ systematically from 1. Following the approach of Iervolino, De Luca, and Cosenza (2010), hypothesis tests are performed for both peak and cyclic EDPs, assuming a lognormal distribution for both response parameters of interest, $\Delta_{\text{inelastic}}$ and N_e. These distribution assumptions were checked with the Shapiro–Wilk test (Shapiro and Wilk, 1965) and could not be rejected at a 95% significance level. The null hypothesis, H_0, is that the median EDPs (the mean of the natural logs of each EDP) for simulated GMs are equal to those from recorded GMs. To address this aim, we selected a two-tails Aspin–Welch test (Welch, 1938) over the standard Student's t-test, as the former does not require the assumption of equal, yet still unknown, variances of populations originating the samples; given the results found, this would be an unreasonable assumption in some cases. The employed test statistic is reported in equation (3), in which z_x and z_y are the sample means, s_x and s_y are the sample standard deviations, and m and n are the sample sizes (in this case, always equal for each earthquake). The test statistic, under H_0, has a Student's t-distribution with the number of degrees of freedom given by Satterthwaite's approximation (Satterthwaite, 1941).

$$t = \frac{z_x - z_y}{\sqrt{\frac{s_x^2}{n} + \frac{s_y^2}{m}}}. \tag{3}$$

A similar parametric hypothesis test, the F-test (e.g., Mood *et al.*, 1974) for normally distributed data, has been performed to compare variances for each EDP (in log terms) for the two datasets (recorded and simulated) corresponding to each earthquake; in this case, the null hypothesis is that the variance of each EDP for simulated GMs is equal to the variance from recorded GMs.

To summarize the results of the hypothesis tests and draw conclusions, the percentages of the hypothesis tests' rejections, assuming a 95% significance level (i.e., choosing an I-type risk, α_I equal to 0.05), are shown in Figures 8 and 9 for each pair (T, R) for $\Delta_{\text{inelastic}}$ and N_e, respectively. In computing these percentages, all of the earthquakes and structural models (EPH and ESD with relative variations) are considered together, yielding a total of 16 cases.

Based on these figures, tests have shown a statistical significance (the percentage of rejections is around 25%) in the bias of the simulated records in terms of median inelastic displacement, only at very short periods and between 1 and 2.5 s, for all of the considered nonlinearity levels (for both EPH and ESD systems). The differences in this period range are likely due to the large differences in both absolute and relative amplitudes (i.e., the shape) of the elastic response for the Loma Prieta and Landers events (Fig. 3). These results confirm that elastic response spectra contain key information related to peak nonlinear response potential, as suggested by past studies on record selection and scaling (e.g., Luco and Bazzurro, 2007).

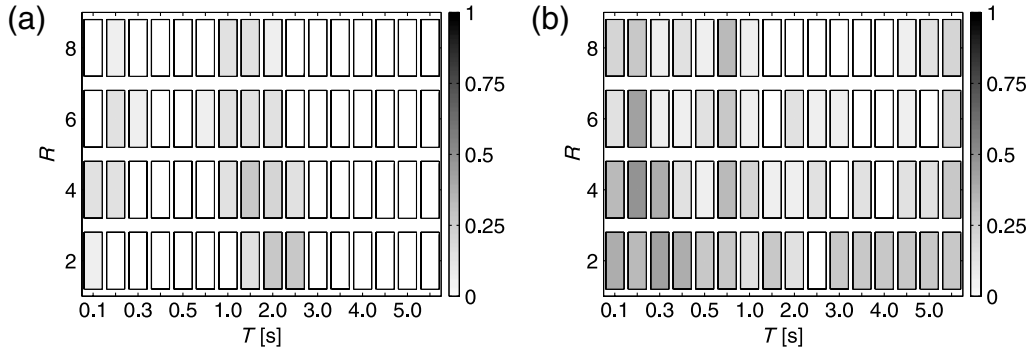

Figure 8. Percentages of hypothesis test rejections ($\alpha_I = 0.05$) for $\Delta_{\text{inelastic}}$; (a) equality of medians and (b) equality of variances.

For equivalent numbers of cycles, the differences found in median and log-standard deviations have statistical significance in the short-period range (<2 s), especially in ESD systems, with some other sparse rejection for very long periods.

In general, these results confirm the considerations based on the visual inspection of Figures 4–7. In some cases, the limited sample size and the relatively large variability may not be able to confirm the hypothesis that the median inelastic spectra generated by simulated GMs (in terms of both $\Delta_{\text{inelastic}}$ and N_e) differ systematically from those produced by recorded GMs at the two customary significance levels (i.e., 5% and 10%).

Sensitivity of the Results to Source-to-Site Distance, Site Conditions, and I_D

This section further discusses the influence of the source-to-site distance and site conditions on the ratios of the medians and log-standard deviations of the inelastic spectra in terms of $\Delta_{\text{inelastic}}$ for simulated and recorded GMs. Specifically, the considered variables are the closest distance to the fault, D (in km), and the shear-wave velocity in the upper 30 m, V_{S30}. Finally, this section investigates the sensitivity of the results, in terms of N_e, to the so-called Cosenza and Manfredi index, I_D (Manfredi, 2001). This dimensionless index I_D has proven to be a good proxy for cyclic structural response (Iervolino *et al.*, 2006); it is defined in equation (4), where $a(t)$ is the acceleration time history, t_E is the total duration of the record, and PGA and PGV are the peak ground acceleration and peak ground velocity, respectively.

$$I_D = \frac{\int_0^{t_E} a^2(t)\mathrm{d}t}{\text{PGA} \cdot \text{PGV}}. \tag{4}$$

Effect of Distance to the Source

Two subsets of 20 and 23 GMs representing two different distance ranges, that is, $D \leq 20$ km and $D > 20$ km, are assembled from the datasets corresponding to the Northridge earthquake (we selected this event because it is characterized by the larger number of stations). For the sake of brevity, only two representative nonlinearity levels, $R = 2$ and $R = 8$, are considered. In particular, Figure 10a shows, in terms of $\Delta_{\text{inelastic}}$, the ratio of the median spectrum from the simulated GMs to the median spectrum from the recorded GMs for each subset (as a function of the period); similarly, Figure 10b shows, in terms of $\Delta_{\text{inelastic}}$, the ratio of the log-standard deviation of the data from the simulated GMs to the log-standard deviation of the data from the recorded GMs for each subset. Figure 10 refers to the EPH model with $\alpha = 3\%$ (to save space, results for the other cases are not presented, although they confirm the findings for this case). Figure 10 shows that, for the range of distances considered in this study, the ratios of the medians do not significantly change

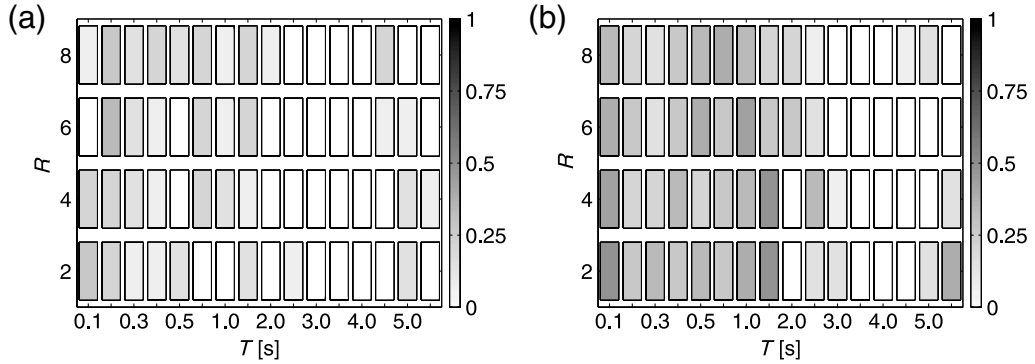

Figure 9. Percentages of hypothesis test rejections ($\alpha_I = 0.05$) for N_e; (a) equality of medians and (b) equality of variances.

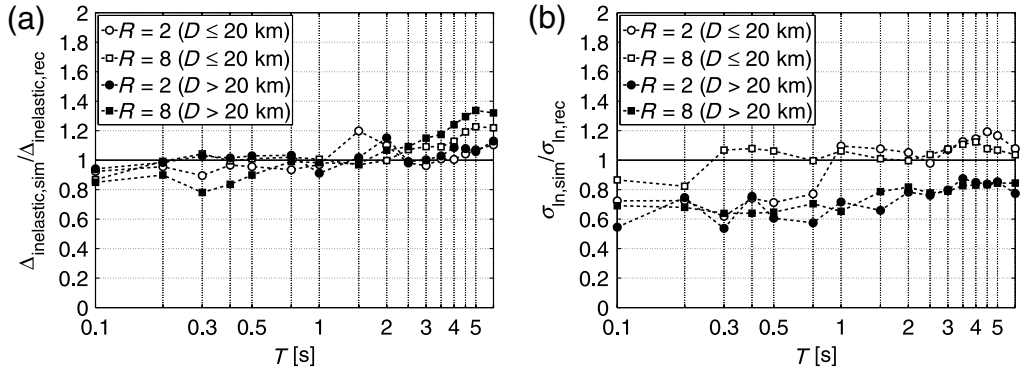

Figure 10. Effect of distance on the ratios of the (a) medians and (b) log-standard deviations of the inelastic spectra (in terms of $\Delta_{\text{inelastic}}$) for simulated GMs to the corresponding quantities computed for the recorded GMs (Northridge earthquake, EPH model with $\alpha = 3\%$).

when computed from GM ensembles representative of different distance ranges for both strong and weak systems (i.e., $R = 2$ and $R = 8$). On the contrary, looking at the ratios of the log-standard deviations for simulated and recorded GMs, moderate and long-period ordinates of both strong and weak systems are significantly influenced by the distance range. In particular, the log-standard deviation of response to simulated records is larger than that of recorded ones across the period range 1–6 s (although, for some periods, the ratio is about 1). As discussed for the Imperial Valley event, this likely can be attributed to the presence in the simulated dataset of GMs featuring strong coherent velocity pulses and then large elastic and inelastic responses. Addressing near-fault effects is the topic of current research; however, it is difficult to precisely quantify and/or calibrate these effects due to the scarcity of recordings close to moderate and large earthquakes. For example, the pulse period classification by Baker (2007) gets at part of this issue. Insights from dynamic rupture simulations (e.g., Schmedes *et al.*, 2010) have the potential to provide additional constraints on the characteristics of the rupture process used in the simulations.

It is evident that strong directivity effects in the simulations need to be studied further. This is needed for validation, and the simulations may also help to refine directivity prediction models.

Effect of Site Class

Two subsets of 16 and 27 GMs representing two different V_{S30} ranges (in m/s), that is, $V_{S30} < 400$ m/s and $V_{S30} \geq 400$ m/s, respectively are assembled from the datasets corresponding to the Northridge earthquake. Also, in this case, only two representative nonlinearity levels, $R = 2$ and $R = 8$, are considered. In particular, Figure 11a shows, in terms of $\Delta_{\text{inelastic}}$, the ratio of the median spectrum from the simulated GMs to the median spectrum from the recorded GMs for each subset (as a function of the period); similarly, Figure 11b shows, in terms of $\Delta_{\text{inelastic}}$, the ratio of the log-standard deviation of the data from the simulated GMs to the log-standard deviation of the data from the recorded GMs for each subset (also, in this case, we refer to the EPH model with $\alpha = 3\%$). For the range of V_{S30} considered in this study, ratios of the medians and log-standard deviations do not change significantly when computed from GM ensembles representative of different V_{S30} ranges for both strong and weak systems (i.e., $R = 2$ and $R = 8$).

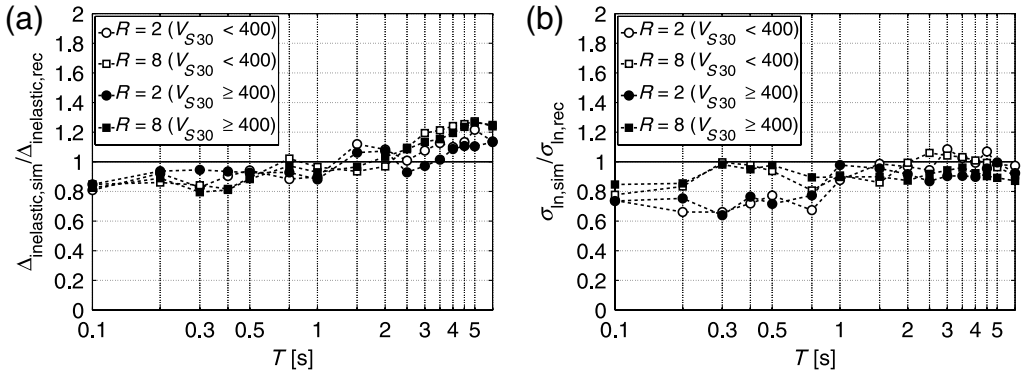

Figure 11. Effect of V_{S30} on the ratios of the (a) medians and (b) log-standard deviations of the inelastic spectra (in terms of $\Delta_{\text{inelastic}}$) for simulated GMs to the corresponding quantities computed for the recorded GMs (Northridge earthquake, EPH model with $\alpha = 3\%$).

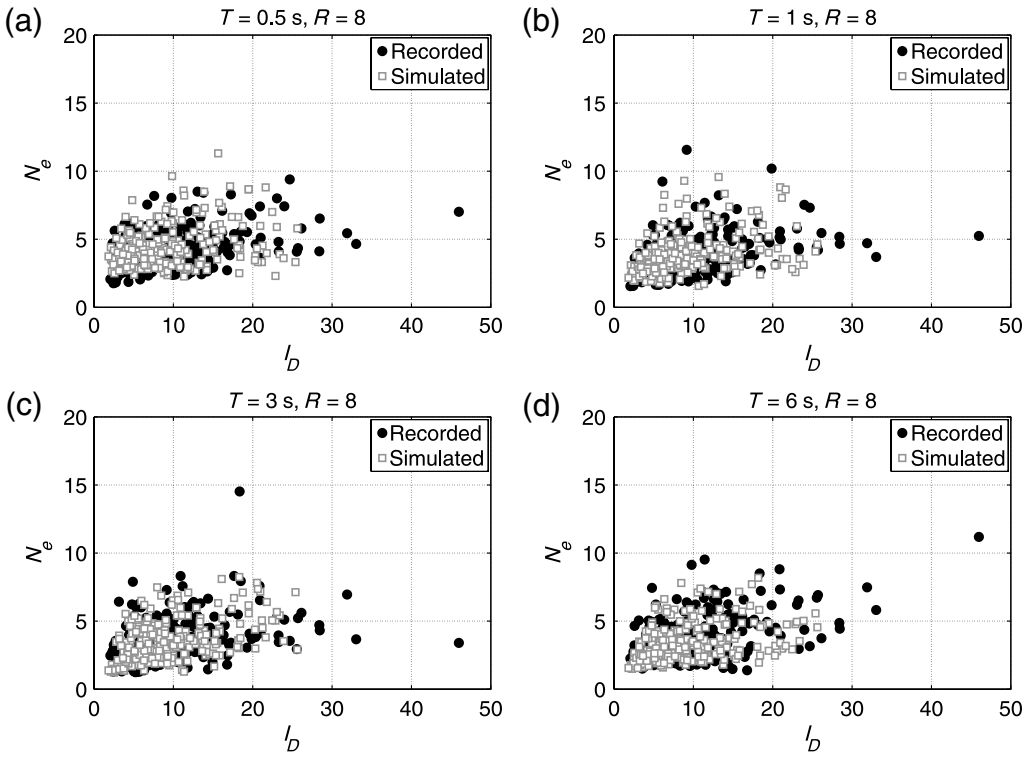

Figure 12. N_e versus I_D ratio for $R = 8$ and different T values (ESD model, $\alpha = 0.10$).

Effect of I_D

Empirical observations and analytical studies show how cyclic structural damage is related to the energy released during ground shaking and then to the duration of a GM. Therefore, each GM has been processed to evaluate its characteristics in terms of integral intensity measure. Figure 12 plots the N_e values for recorded and simulated datasets as a function of I_D; all of the parts of Figure 12 consider all of the earthquakes together. For the sake of brevity and based on the findings presented in the Results and Discussion section, only results for ESD systems with $\alpha = 10\%$ are presented (results for EPH systems are substantially equivalent). Four representative periods of 0.5, 1, 3, and 7 s are considered alongside the highest nonlinearity level, $R = 8$. The conclusions here hold for all other SDoF cases.

Figure 12 reveals that the simulation closely matches both the level and trend of the observed values (i.e., N_e to recorded GMs) as a function of I_D, although a lower variability is evident in the N_e values produced by the simulated GMs. Moreover, looking at the integral (duration-related) intensity measures characterizing each record, a fairly good correlation between the two parameters confirms that differences in cyclic response may be predictable (e.g., Iervolino *et al.*, 2006). In fact, a two-tails Aspin–Welch test has been performed to check equality between average I_D values for the two datasets (null hypothesis), recorded and simulated, corresponding to each earthquake. Except for the Imperial Valley, the resulting p values are smaller than 0.05 (i.e., 0.004 for Loma Prieta, and 0.04 for Landers and Northridge), rejecting the null hypothesis. This result explains the good match between the cyclic response (in terms of N_e) of the simulations and observations for Imperial Valley, as well as the differences found for Loma Prieta, Landers, and Northridge.

Conclusions

The design of new structures or assessment of existing ones may be complicated by the limited number or total absence of suitable real (i.e., recorded) accelerograms for the earthquake scenarios that dominate the seismic hazard at a given site. Therefore, hybrid broadband synthetic records may be an attractive alternative as input to nonlinear dynamic analysis if their structural response equivalency to real GMs with the same seismological features is proven.

The present study had two main objectives: (1) to validate the hybrid broadband simulation methodology of Graves and Pitarka (2010) by statistically examining post-elastic peak and cyclic responses caused by both simulated and recorded GMs for past events and (2) to identify situations where the simulated and recorded GMs produce different response characteristics to determine additional areas where refinement in the simulations is needed. The validation methodology was based on structural engineering demand metrics (of interest in performance-based earthquake engineering) and a formal statistical approach.

The studies investigated SDoF systems with different force–displacement backbones and hysteretic rules at different nonlinearity levels and for several fundamental periods. The maximum inelastic displacement and the equivalent number of cycles response of 272 systems were analyzed with respect to recorded and simulated GMs for four historical earthquakes: 1979 M_w 6.5 Imperial Valley, 1989 M_w 6.8 Loma Prieta, 1992 M_w 7.2 Landers, and 1994 M_w 6.7 Northridge. From a broader perspective, the simulation methodology of the study provides a complete prescription for simulating motions for future earthquakes, including extrapolation to those beyond the magnitude ranges considered in the current set of validation events. This is one of the main objectives in developing any type of simulation model: to fully exploit its predictive capability.

The results of this study show, in the context of the SDoF systems studied, that the simulation methodology matches well the median peak seismic demands produced by recorded GMs and that the observed differences generally are not statistically significant across the entire frequency bandwidth. However, for certain structural systems, simulated accelerograms may produce median inelastic demands that differ from a similar estimate using corresponding recorded motions, and these differences are statistically significant. In particular, the simulation appears to be especially biased in the transition area between semistochastic and deterministic simulations for the Loma Prieta and Landers events (around 1 s). The observed differences are due to systematic differences in the average shape around those periods of the linear response spectra generated by synthetic and real GMs, confirming that spectral shape is a key parameter in record selection.

In addition, some systematic differences are observed in cyclic response, mostly in the short-period range where the simulation is semistochastic. The observed differences are likely due to systematic differences in the integral GM parameters for each dataset (in particular, the Cosenza and Manfredi index), which are strongly correlated with the inelastic cyclic response.

For all events considered in this study, the intraevent dispersion in the structural response due to the simulation is generally lower than that for recorded GMs at short periods. This result is consistent with the findings of Star *et al.* (2011), who found that the Graves and Pitarka (2010) methodology produced less intraevent variability in shorter-period ground motions compared with GMPEs. At longer periods, the simulations can generate strong velocity pulses at sites experiencing forward rupture directivity. These pulses produce larger long-period elastic and inelastic demands in comparison with recorded GMs, causing the simulation to overestimate intraevent variability. This suggests that the rupture characterization procedure used in the simulations for some events (e.g., Imperial Valley and Northridge) may need further refinement to reduce the level of coherency in the rupture process.

This paper's generally favorable comparisons between simulations and recorded data lend support to the predictive capabilities of the simulation methodology, and are directly relevant to the engineering community, who may use the simulation methodology with trust. These results may also provide feedback for seismologists who generate simulated GMs for engineering applications.

Data and Resources

The simulated ground-motion waveform data used in this study were obtained from the electronic supplement to Graves and Pitarka (2010; last accessed December 2011). The NGA strong-motion data came from the Pacific Earthquake Engineering Research (PEER) Ground Motion Database, available at http://peer.berkeley.edu/peer_ground_motion_database (last accessed December 2011). The Southern California Earthquake Center (SCEC) Broadband Platform is available at http://scec.usc.edu/research/cme/groups/broadband (last accessed June 2012).

Acknowledgments

This research was supported by Rete dei Laboratori Universitari di Ingegneria Sismica (ReLUIS) for the research program founded by the Italian Department of Civil Protection—Executive Project 2010–2013, and by the National Science Foundation (NSF)-sponsored Southern California Earthquake Center (SCEC) through the Technical Activity Group (TAG) on Ground Motion Simulation Validation (GMSV). Their support is gratefully acknowledged. Any opinions, findings, conclusions, and recommendations expressed in this paper are those of the authors and do not necessarily reflect the views of the sponsors.

Constructive and insightful comments and suggestions by two anonymous reviewers and Nicolas Luco and Brad Aagaard of the U.S. Geological Survey (USGS) were very helpful in improving the paper.

References

American Society of Civil Engineering (ASCE) (2010). Minimum design loads for buildings and other structures (7–10), *Standards ASCE/SEI 7-10*.

Atkinson, G. M., and K. Goda (2010). Inelastic seismic demand of real versus simulated ground motion records for the Cascadia subduction earthquakes, *Bull. Seismol. Soc. Am.* **100,** no. 1, 102–115.

Baker, J. W. (2007). Quantitative classification of near-fault ground motions using wavelet analysis, *Bull. Seismol. Soc. Am.* **97,** no. 5, 1486–1501.

Baker, J. W., and N. Jayaram (2008). Validation of ground motion simulations for engineering applications, in *Proc. of the Southern California Earthquake Center (SCEC) Annual Meeting*, Palm Springs, California, 6–11 September.

Bazzurro, P., B. Sjoberg, and N. Luco (2004). Post-elastic response of structures to synthetic ground motion, *Report for Pacific Earthquake Engineering Research (PEER) Center Lifelines Program Project*, Report 1G00 Addenda, 65–112.

Bazzurro, P., B. Sjoberg, N. Luco, W. Silva, and R. Darragh (2004). Effects of strong motion processing procedures on time histories, elastic and inelastic spectra, in *Proc. of the Invited Workshop on Strong-Motion Record Processing*, Richmond, California, 26–27 May.

Campbell, K. W., and Y. Bozorgnia (2008). NGA ground motion model for the geometric mean horizontal component of PGA, PGV, PGD and 5% damped linear elastic response spectra for periods ranging from 0.01 to 10 s, *Earthq. Spectra* **24,** no. 1, 139–171.

Graves, R. W., and B. T. Aagaard (2011). Testing long-period ground-motion simulations of scenario earthquakes using the M_w 7.2 El Mayor–Cucapah mainshock: Evaluation of finite-fault rupture

characterization and 3D seismic velocity models, *Bull. Seismol. Soc. Am.* **101,** no. 2, 895–907.

Graves, R. W., and A. Pitarka (2010). Broadband ground-motion simulation using a hybrid approach, *Bull. Seismol. Soc. Am.* **100,** no. 5A, 2095–2123.

Haselton, C. B. (Editor) (2009). Evaluation of ground motion selection and modification methods: Predicting median interstory drift response of buildings, *PEER Report 2009/01*, Pacific Engineering Research Center, University of California, Berkeley, California.

Ibarra, L. F., R. A. Medina, and H. Krawinkler (2005). Hysteretic models that incorporate strength and stiffness deterioration, *Earthq. Eng. Struct. Dynam.* **34,** no. 12, 1489–1511.

Iervolino, I., F. De Luca, and E. Cosenza (2010). Spectral shape-based assessment of SDoF nonlinear response to real, adjusted and artificial accelerograms, *Eng. Struct.* **32,** no. 9, 2776–2792.

Iervolino, I., C. Galasso, and E. Cosenza (2010). REXEL: Computer aided record selection for code-based seismic structural analysis, *Bull. Earthq. Eng.* **8,** no. 2, 339–362.

Iervolino, I., C. Galasso, R. Paolucci, and F. Pacor (2011). Engineering ground motion record selection in the ITalian ACcelerometric Archive, *Bull. Earthq. Eng.* **9,** 1761–1778.

Iervolino, I., G. Manfredi, and E. Cosenza (2006). Ground-motion duration effects on nonlinear seismic response, *Earthq. Eng. Struct. Dynam.* **35,** no. 1, 21–38.

Luco, N., and P. Bazzurro (2007). Does amplitude scaling of ground motion records result in biased nonlinear structural drift responses?, *Earthq. Eng. Struct. Dynam.* **36,** no. 13, 1813–1835.

Manfredi, G. (2001). Evaluation of seismic energy demand, *Earthq. Eng. Struct. Dynam.* **30,** no. 4, 485–499.

Mood, M. A., F. A. Graybill, and D. C. Boes (1974). Introduction to the Theory of Statistics, Third Ed., McGraw-Hill, New York, 480 pp.

Naeim, F., and R. W. Graves (2006). The case for seismic superiority of well-engineered tall buildings, *Struct. Des. Tall Spec. Build.* **14,** no. 5, 401–416.

Olsen, K. B., and J. E. Mayhew (2010). Goodness-of-fit criteria for broadband synthetic seismograms, with application to the 2008 M_w 5.4 Chino Hills, California, earthquake, *Seismol. Res. Lett.* **81,** no. 5, 715–723.

Olsen, K. B., S. M. Day, and C. R. Bradley (2003). Estimation of Q for long-period (>2 s) waves in the Los Angeles Basin, *Bull. Seismol. Soc. Am.* **93,** no. 2, 627–638.

Rezaeian, S., and A. Der Kiureghian (2011). Simulation of orthogonal horizontal ground motion components for specified earthquake and site characteristics, *Earthq. Eng. Struct. Dynam.* **41,** no. 2, 335–353.

Satterthwaite, F. E. (1941). Synthesis of variance, *Psychometrika* **6,** no. 5, 309–316.

Schmedes, J., R. J. Archuleta, and D. Lavallée (2010). Correlation of earthquake source parameters inferred from dynamic rupture simulations, *J. Geophys. Res.* **115,** doi: 10.1029/2009JB006689.

Shapiro, S. S., and M. B. Wilk (1965). An analysis of variance test for normality (complete samples), *Biometrika* **52,** nos. 3–4, 591–611.

Somerville, P. G. (1993). Engineering applications of strong ground motion simulation, *Tectonophysics* **218,** nos. 1–3, 195–219.

Star, L., J. P. Stewart, and R. W. Graves (2011). Comparison of ground motions from hybrid simulations to NGA prediction equations, *Earthq. Spectra* **27,** no. 2, 331–350.

Stewart, J. P., E. Seyhan, and R. W. Graves (2011). Calibration of a semi-stochastic procedure for simulating high frequency ground motions, *PEER Report 2011/09*, Pacific Engineering Research Center, University of California, Berkeley, California.

Vanmarcke, E. H., G. A. Fenton, and E. Heredia-Zavoni (1997). *SIMQKE-II, Conditioned Earthquake Ground Motion Simulator: User's Manual, version 2*, Princeton University, Princeton, New Jersey, 25 pp.

Veletsos, A. S., and N. M. Newmark (1960). Effect of inelastic behavior on the response of simple systems to earthquake motions, in *Proc. of 2nd World Conference on Earthquake Engineering*, Tokyo and Kyoto, Japan, 11–18 July 1960 Vol. 2, 895–912.

Welch, B. L. (1938). The significance of the difference between two means when the population variances are unequal, *Biometrika* **29,** 350–362.

Department of Civil and Environmental Engineering
University of California, Irvine
E/4141 Engineering Gateway Building
Irvine, California 92697-2175
(C.G., F.Z.)

Dipartimento di Ingegneria Strutturale
Università degli Studi di Napoli Federico II
via Claudio 21
Naples 80125
Italy
(I.I.)

U.S. Geological Survey
Earthquake Science Center
Pasadena Field Office
525 South Wilson Ave.
Pasadena, California 91106
(R.W.G.)

Manuscript received 14 January 2012